Controlled Positioning of Large Interfacial Nanocavities via Stress-Engineered Void Localization**

Firat Güder, Yang Yang,* Silvana Goetze, Andreas Berger, Niranjan Ramgir, Dietrich Hesse, and Margit Zacharias*

The Kirkendall effect has intensively been exploited at the nanoscale for the fabrication of hollow nanostructures.[1,2] This fabrication strategy generally starts from a core–shell nanostructure where the core material is a faster diffusing species. Preferred outward atomic diffusion across the interface leads to a net inward injection of vacancies, which are likely to accumulate, supersaturate, and finally condense into a single void. If the core material is only partly consumed, a core–void–shell nanostructure can be produced.[3–7] Investigations on the formation of this ''intermediate'' state are crucial for a deep understanding of the vacancy coalescence and void evolution process induced by the nanoscale Kirkendall effect. Moreover, nanostructures with controlled porosity would enable greater control of the local chemical environment, which is important for molecule probing, drug delivery and catalysis applications.[2–4]

Generally the nucleation of Kirkendall voids is favored at a core–shell interface due to the high defect content and stress there. In most cases of spherical core–shell nanoparticles, uniformly distributed interfacial voids are divided by filament-like bridges, which act as fast transport paths for the delivery of remaining core material into the shell.[2a,2f,4] In materials with one or more macroscopic dimensions such as nanowires and films, the nanoscale Kirkendall effect usually initiates the formation of multiple voids randomly scattered at the interface during the diffusion evolution.[5] Void localization has been noticed in some systems.[5b,6,7] For example, an asymmetric intermediate structure was observed during sulfidation of cadmium nanocrystallites, where the unreacted cadmium core and the coalesced vacancies were separated into two distinct spherical caps.[6] This void positioning was attributed to the greater metal/vacancy self-diffusivities in the core compared to the diffusivity of the cations through the shell. However, the question still remains whether one can actually design hollow nanostructures by intentionally positioning locally arranged nanovoids and nanochannels.

Here, we suggest a flexible stress-mediated approach to spatially define the localization of large Kirkendall voids in low-symmetry systems. We select ZnO/Al_2O_3 core–shell nanowires and ZnO/Al_2O_3 multilayer structures as examples to illustrate our strategy. The ZnO/Al_2O_3 thermal diffusion couple has two advantages for such a case study: first, the solid–solid $ZnAl_2O_4$-forming reaction between ZnO and Al_2O_3 involves one-way diffusion of ZnO into Al_2O_3, which represents an extreme case of the Kirkendall effect.[2d] Thus, the influence of interdiffusion can be ignored. Second, given that the thickness of the Al_2O_3 shell can be well tuned by atomic layer deposition (ALD), the extent of reaction can be premeditated.

ZnO nanowires synthesized via a vapor transport (vapor–solid) method were first coated with a uniform 12 nm amorphous Al_2O_3 film by ALD. The diameter of the ZnO nanowires ranges from 50 to 200 nm, which is more than enough for the complete consumption of the 12 nm thin Al_2O_3 shell in the $ZnAl_2O_4$-forming reaction. Figure 1a shows an underfocus transmission electron microscopy (TEM) image of this sample after annealing at 600 °C for 15 h. It is found that small spherical voids are uniformly dispersed at the surface of the ZnO nanowire core. Our previous work has revealed that the sufficient formation of $ZnAl_2O_4$ by solid state reaction of ZnO/Al_2O_3 core–shell nanowires requires a temperature window above 700 °C.[8b] Therefore, annealing at a lower temperature such as 600 °C can only initiate a partial diffusion reaction.[8] The uniform void distribution shown in Figure 1a indicates the homogeneous nucleation and growth of initial Kirkendall voids. In addition, it is noticed that those voids, which formed at the interface close to the nanowire tip, are inclined to fuse into relatively large ones (inset in Figure 1a).

When the annealing was performed at 700 °C for 5 h, multiple voids with large sizes appeared at the interface as a result of the adequate outward diffusion of ZnO accompanying the complete transformation of the Al_2O_3 shell into $ZnAl_2O_4$ (Figure 1b). The formation of the multiple voids indicates that the vacancies in ZnO lack sufficient mobility to diffuse over a long distance. In the case of two-component systems, the

[*] F. Güder, Dr. Y. Yang, Dr. N. Ramgir, Prof. M. Zacharias
Nanotechnology Group
Institute of Microsystems Engineering (IMTEK)
Albert-Ludwigs-University Freiburg
Georges-Köhler-Allee 103, 79110 Freiburg (Germany)
E-mail: gueder@imtek.de; yang.yang@imtek.de
Dr. Y. Yang, S. Goetze, Dr. A. Berger, Prof. D. Hesse
Max Planck Institute of Microstructure Physics
Weinberg 2, 06120 Halle (Germany)

[**] We thank Dr. T. Y. Tan, K. Subannajui, A. Baur, and M. Reichel for their assistance in sample preparation and Dr. R. Scholz for part of the TEM observations. This work was supported by Deutsche Forschungsgemeinschaft (DFG) under contracts ZA 131/23-1 (Freiburg) and HE 2100/8-1 (Halle).

Supporting Information is available on the WWW under http://www.small-journal.com or from the author.

DOI: 10.1002/smll.201000561

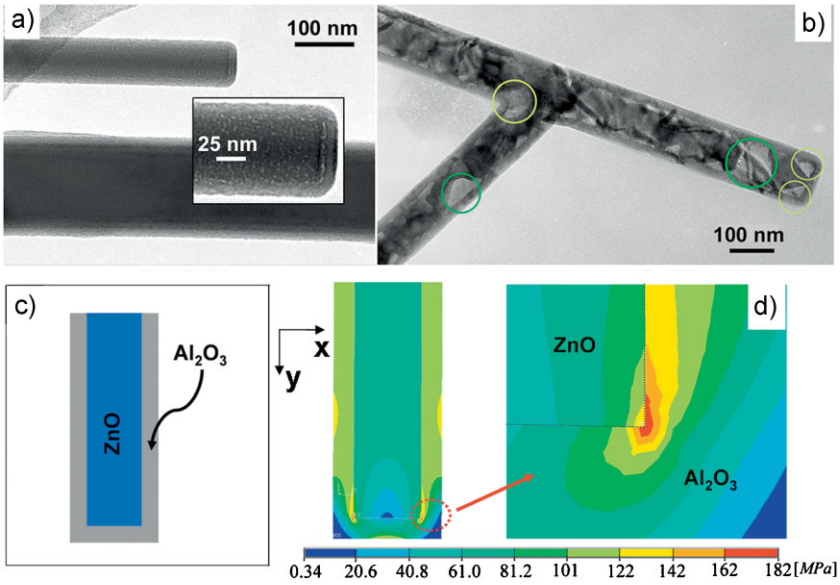

Figure 1. a) Underfocus TEM image of ZnO nanowires with a 12-nm-thick Al_2O_3 shell after annealing at 600 °C for 15 h; b) TEM image of ZnO nanowires with a 12-nm-thick Al_2O_3 shell after annealing at 700 °C for 5 h (The Al_2O_3 shell was completely transformed into $ZnAl_2O_4$ after annealing); c) Geometry of the tip of a ZnO/Al_2O_3 core–shell nanowire; d) Simulated stress distribution at the tip of a ZnO/Al_2O_3 nanowire due to thermal expansion at 700 °C. The diameter of the core is 40 nm while the thickness of the shell is 12 nm.

diffusion process is controlled by the slower diffusing species. For metal oxides such as ZnO, oxygen always has a lower diffusion coefficient. An effective mobility of oxygen requires a diffusion coefficient up to 10^{-22} $m^2 \cdot s^{-1}$.[5b] However, the self-diffusivity of oxygen in ZnO at 700 °C is 2–3 orders of magnitude lower than this value.[9] Therefore, the localization of the interfacial voids in the ZnO/Al_2O_3 core–shell nanowires cannot be achieved by void coalescence via a long-range migration.[6]

The "faceted", crystallographic shape of the interfacial voids formed at 700 °C demonstrates that the surface diffusion on the ZnO core is a dominant mass flow mode responsible for the enlargement of the Kirkendall voids.[5a] Since the surface diffusion of ZnO presents a faster kinetics for the void growth,[10] a finally evolved void with a larger size is supposed to develop from an initial Kirkendall void whose nucleation is preferred. As seen from Figure 1b, although some large voids are occasionally encountered on the stem (marked by green circles), the voids located at the corners and curved boundaries (marked by yellow circles) are generally a little bigger than most of the others, agreeing with the observation from the reaction at 600 °C. This enhanced reactivity and diffusivity at corners of the core–shell interface can be ascribed to the enhanced applied force induced by geometry.

The effects of stress on atomic diffusion and vacancy accumulation can be explained with a modified version of Fick's first law:[11]

$$J = D[-\nabla c - \frac{c\nabla V}{kT}] \quad (1)$$

where J is the flux of atoms, k the Boltzmann constant, T the temperature, c the concentration of the atoms, D the diffusion coefficient, and ∇V is the potential gradient of the force. This equation describes an atomic diffusion process when a potential gradient of force exists in addition to a concentration gradient. The term $\frac{-c\nabla V}{kT}$ indicates that in the presence of a stress field created by an applied force, diffusion of atoms occurs along the negative stress gradient.

Generally sharp corners greatly increase the stress concentration. This high amount of stress concentration can often lead to failure of plastic parts.[12] It is well known that the failure of many bi- and multi-material joints initiates from one or more interface corners. For lattice-mismatched core–shell nanowires, it is revealed that the stress distribution in their interior is very inhomogeneous. While the details vary from sample to sample, the stress maxima in the core usually occur in the corner region at the core–shell interface.[13] Figure 1c,d shows the geometry of the tip of a ZnO/Al_2O_3 core–shell nanowire and a 2D simulation of its stress distribution caused by thermal expansion at 700 °C (Supporting Information).[14] The simulation result indicates that the highest stress in the ZnO core appears at the interfacial corners, in agreement with other core–shell nanowire systems previously reported.

When the ZnO core reacts with the amorphous Al_2O_3 shell at high temperatures through the nanoscale Kirkendall effect, the nearly identical concentration gradient of ZnO along the core–shell interface should induce a uniform void evolution at various sites. However, the large stress created on the corners can enhance the diffusion of ZnO away from these areas. This in turn enhances the vacancy flux towards this position. Also, the low radius of curvature favors outward diffusion of the core material. Therefore, vacancies more easily supersaturate and coalesce into voids at the corner. These preferentially nucleated voids will merge, grow, and finally evolve into "faceted" voids by kinetically favorable surface diffusion. Their final size should be larger than the size of those developed during a long nucleation period. Note that defects such as grain boundaries and cracks formed during the shell growth can also favor the outward diffusion of core material.[15] This is the reason why we found some large voids along the stem as well (Figure 1b). However, the formation of the defects that can act as preferential nucleation sites for Kirkendall voids is stochastic. Basically the defect profile of the nanostructure is difficult to modulate.

Regarding the diffusion process in the presence of a stress field described in Equation (1), the contribution from the stress gradient can be prominent only if its magnitude is comparable to that from the concentration gradient. If the concentration gradient is very high, the influence of the stress might be hidden. Alivisatos's group once investigated the sulfidation of disk-shaped cobalt particles in solution.[4a] A stress-mediated effect was not observed though anticipated. This outcome might be

caused by a continuously high concentration gradient of cobalt between the inside and outside of the shell. This assumption is reasonable because of the high concentration of sulfur in solution, which can be regarded as a sink for the diffusing cobalt cations. In our case of ZnO nanowires coated by a 12-nm-thick Al_2O_3 shell, the stress effect on diffusion is observed, but still insufficient for the formation of large interfacial nanocavities localized at the high-stress positions (Figure 1b and Supporting Information, Figure S1). For magnifying the role of stress, there are two possible routes based on Equation (1): decreasing the concentration gradient of the diffusing material or increasing the stress gradient at intended positions.

Firstly, we deposited a uniform 3-nm-thick Al_2O_3 film on the ZnO nanowires by ALD instead of the original 12-nm-thick shell. After annealing at 700 °C for 5 h, a very large interfacial nanocavity was exclusively formed at the tip of each core–shell nanowire, as shown in Figure 2a. Along the stem very small voids are observed in most cases. In contrast to the result shown in Figure 1b, the reduction of thickness of the Al_2O_3 shell leads to a much more preferential void formation at the tips. It can be assumed that, once the reaction between the ZnO nanowire core and the 3-nm-thick Al_2O_3 shell started, the concentration gradient of ZnO across the interface and the shell decreased more rapidly due to the reduced diffusion space for Zn^{2+} and O^{2-}. As a result, the geometry-induced stress influences the diffusion of ZnO and the nucleation of the Kirkendall voids to a greater degree. Finally, a big void is positioned at the region of the highest induced stress. In view of the cavity size located at each end, the ''loss'' of the excess ZnO is high during the formation of the encapsulating $ZnAl_2O_4$ shell. This observation indicates that longitudinal diffusion of ZnO in the Al_2O_3 shell also occurred during the void enlargement by surface diffusion.

In the second experiment, a 12-nm-thick Al_2O_3 film was deposited on gold-capped ZnO nanowires synthesized by a vapor–liquid–solid mechanism (Figure 2b), where gold was used as a catalyst. After reaction at 700 °C for 5 h, we typically observe a hollow section at the gold/nanowire interface, as shown in Figure 2c. In comparison with the 12-nm-thick Al_2O_3 film on the ZnO nanowires without a gold cap, the introduction of gold obviously accelerates the diffusion of the adjacent ZnO nanowire core atoms. The gold/nanowire interface is a region of high stress due to large curvature and lattice mismatch.[16] Therefore, the contribution from the concentration gradient was ''weakened'' by addition of a very large stress gradient, the value of which is unattained only by the corner geometry of the ZnO/Al_2O_3 core–shell nanowires.

Using the stress effect on Kirkendall void formation, novel $ZnAl_2O_4$ nanotubes with embedded ZnO nanocrystals were synthesized from diameter oscillatory ZnO/Al_2O_3 core–shell nanowires. ZnO nanowires with diameter oscillation were fabricated via a vapor transport route (Supporting Information, Figure S2). Figure 2d,e shows TEM images of 12-nm-thick Al_2O_3 coated rippled ZnO nanowires before and after annealing, respectively. After annealing at 700 °C for 5 h, the diameter oscillatory core–shell nanowires were transformed into a so-called pea-pod structure (see also the Supporting Information, Figure S3). Large nanocavities are only observed in areas where the nanowires are constricted to smaller diameters, which separate the remaining ZnO nanowire core into unconnected ''nanopeas'' (Supporting Information, Figure S4 and S5). The rippled nanostructure indeed creates an oscillating stress field with a periodic fluctuation by thermal expansion. Its stress gradient is higher in the narrower sections of the nanowires compared to the wider sections.[17] Consequently, the void nucleation is more favorable at these positions and the pea-pod nanostructure is formed.

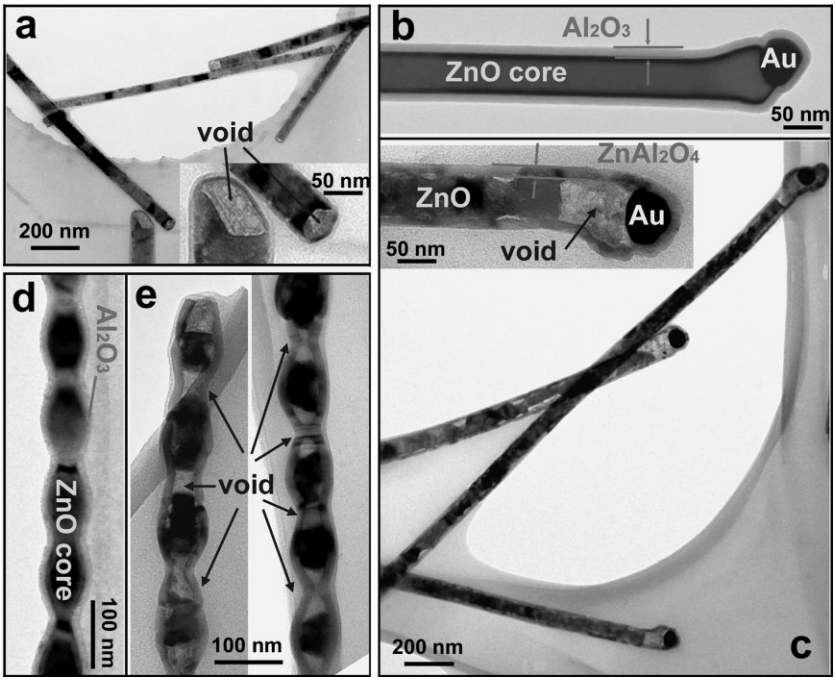

Figure 2. TEM images of a) ZnO nanowires with a 3-nm-thick Al_2O_3 shell after annealing at 700 °C for 5 h; gold-capped ZnO nanowires with a 12-nm-thick Al_2O_3 shell before (b) and after (c) annealing at 700 °C for 5 h; diameter oscillatory ZnO nanowires with a 12-nm-thick Al_2O_3 shell before (d) and after (e) annealing at 700 °C for 5 h. All the Al_2O_3 shells were transformed into $ZnAl_2O_4$ after annealing.

Furthermore, we tested this stress-mediated void localization strategy by comparing plane ZnO/Al_2O_3 multilayer structures and the same multilayers gown over V-trenches. Figure 3a illustrates an overview of the two types of multilayers including five Al_2O_3 and four ZnO layers periodically deposited by ALD on flat silicon substrates and silicon V-trenches (Supporting Information, Figure S6). The thickness of each Al_2O_3 and ZnO layer is 24 and 12 nm, respectively. After the solid–solid $ZnAl_2O_4$ forming reaction, disconnected Kirkendall channels/voids were formed in the multilayer between the $ZnAl_2O_4$ layers on the flat substrates after annealing at 700 °C for 3 h (Figure 3b). The voids are distributed without a pattern, similar to the result of concentration-

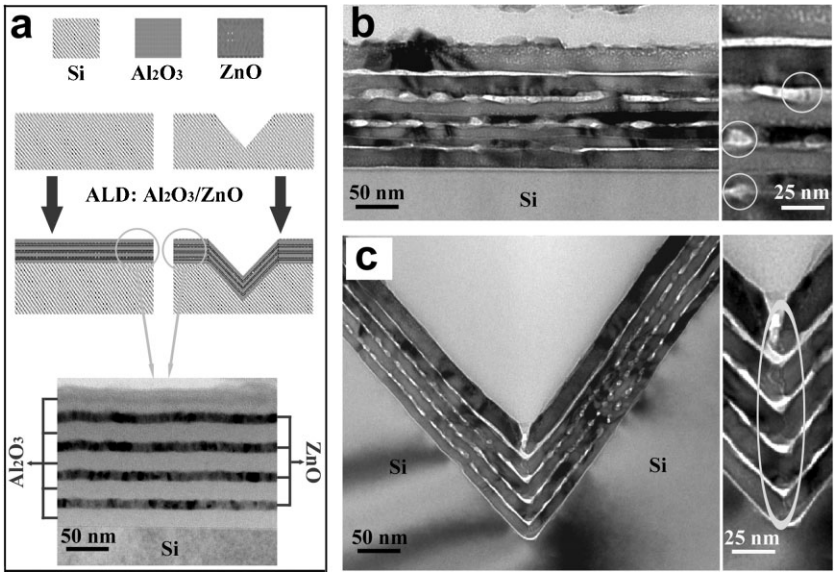

Figure 3. a) Process flow for the preparation of ZnO/Al_2O_3 multilayers on flat silicon substrates and silicon V-trenches; Cross-sectional TEM images of $ZnAl_2O_4$ multilayers formed by ZnO/Al_2O_3 solid–solid reaction at 700 °C for 3 h on b) flat silicon substrates and c) silicon V-trenches.

dominated one-way diffusion of ZnO in ZnO/Al_2O_3 core–shell nanowires. The Al_2O_3/ZnO multilayer deposited on Si V-trenches shows a significantly different void morphology upon annealing. As seen in the TEM image in Figure 3c, large voids are always pinned at the bottom of the V-trench while unordered smaller voids are distributed elsewhere in the structure.

The larger stress especially for the top Al_2O_3 layer revealed by simulation (Supporting Information, Figure S7) might result in a symmetric cracking at the bottom corner of the top layer. The stress generated through the conversion of Al_2O_3 to $ZnAl_2O_4$ can further aggravate the fracture. The surface of the crack will enhance the diffusion of the top ZnO layer along the crack line and explains partly the large voids there. The embedded layers below do not have such cracking but still an accumulation of voids is observed at the bottom corner of the V-trenches. Due to the geometry of the multilayer V-trench structure and the different thermal expansion coefficients of the two materials, small regions of reduced stress in the bottom corners of the ZnO layers alternate with regions of enhanced stress in the bottom corners of the alumina layers (Supporting Information, Figure S7). In addition, a high stress gradient exclusively appears in each ZnO layer adjacent to its bottom. Thus a periodic stress pattern is formed along the symmetry line (face) of the V-groove area of the deposited multilayer. Obviously this periodic pattern results in a preferred nucleation of voids along this symmetry line (face), and their subsequent preferred growth. We suggest that such stress-engineered strategies will provide a potential route to fabricate continuous nanochannels in multilayer structures based on the nanoscale Kirkendall effect.

In summary, we investigated the effect of stress on the void nucleation during ZnO/Al_2O_3 solid–solid reaction through the nanoscale Kirkendall effect. Based on a stress-assisted diffusion process, new nanostructures with positioned large interfacial nanocavities were fabricated. Our results demonstrate that the stress engineered diffusion mechanism in combination with the Kirkendall effect can be used to specifically design hollow nanostructures. This void engineering strategy can be further extended to other thermal diffusion couples.

Experimental Section

Nanowires were grown by a vapor-phase deposition technique on silicon or GaN/sapphire substrates using gold dots as catalyst. For nanowire growth, ZnO (Sigma Aldrich 99.999%) and graphite (Alfa/Aesar ≈200 mesh) powders were mixed in a 1:1 ratio and placed inside a quartz tube furnace along with the substrates. The tube pressure and temperature were kept at 200 mbar and 875–939 °C, respectively, during growth. A mixture of O_2 (0.001 sccm) and Ar (7 sccm) was used as the carrier gas in the tube furnace. The growth mode from vapour–solid to vapour–liquid–solid is switched intentionally.

"V" shaped trenches on Si (100) substrates were formed by first depositing an etch mask of 400-nm SiO_2 and 110-nm Si_3N_4 via low-pressure chemical vapor deposition (LPCVD) on a Si (100) wafer and then structuring the etch mask by conventional lithography, reactive ion etching processes and dipping the wafer in 30% KOH solution for anisotropic wet etching. Upon the completion of the wet-etching process, the etch mask was stripped in buffered HF solution (Supporting Information, Figure S6). After etch-mask stripping, both the flat and the structured Si substrates were treated with piranha solution to remove any contaminants from the surface and then dipped in 1% HF to remove the chemically formed SiO_2.

ZnO nanowires coated with a 12- or 3-nm-thick Al_2O_3 shell and Al_2O_3/ZnO multilayer structures, consisting of four periods of Al_2O_3 and ZnO, ending with an additional top Al_2O_3 layer, were grown by atomic layer deposition at 150 °C (Oxford Instruments, OpAL). For the Al_2O_3/ZnO multilayer, the thickness of each layer was precisely controlled by the number of diethylzinc (DEZ)/H_2O and trimethylaluminum (TMA)/H_2O exposure cycles. The dosing time for DEZ and TMA was set to 40 ms and 20 ms, respectively, with 20 ms of H_2O for both of the exposure cycles. The deposition chamber was pumped down to 8 mTorr before the process and kept between 170–190 mTorr during the process. The chamber was purged with N_2 for 10 s after each precursor pulse to remove any residual gases to prevent parasitic reactions. Thicknesses of Al_2O_3 and ZnO layers were 24 nm and 12 nm, respectively.

All samples (nanowires and films) were annealed in a horizontal quartz tube furnace with open ends at a temperature of 700 or 600 °C. The annealing time was changed from 3 to 15 h.

The TEM samples were characterized and analyzed using TEM (JEOL, JEM-1010; Philips, CM20T). Energy-dispersive X-ray (EDX) spectroscopy was performed using a Philips CM20FEG scanning TEM instrument equipped with an EDX detector (IDFix-system, SAMx). Scanning electron microscopy (SEM) observations were carried out by using a FEI Nova NanoSEM 430.

Keywords:
solid state reaction · interfacial reaction · stress gradient · nanocavities · void localization

[1] A. D. Smigelskas, E. O. Kirkendall, *Trans. AIME* **1947**, *171*, 130.
[2] a) Y. Yin, R. M. Rioux, C. K. Erdonmez, S. Hughes, G. A. Somorjai, A. P. Alivisatos, *Science* **2004**, *304*, 711; b) Y. Wang, L. Cai, Y. Xia, *Adv. Mater.* **2005**, *17*, 473; c) Q. Li, R. M. Penner, *Nano Lett.* **2005**, *5*, 1720; d) H. J. Fan, M. Knez, R. Scholz, K. Nielsch, E. Pippel, D. Hesse, M. Zacharias, U. Gösele, *Nat. Mater.* **2006**, *5*, 627; e) R. K. Chiang, R. T. Chiang, *Inorg. Chem.* **2007**, *46*, 369; f) S. Peng, S. Sun, *Angew. Chem.* **2007**, *119*, 4233; *Angew. Chem. Int. Ed.* **2007**, *46*, 4155; g) H. J. Fan, U. Gösele, M. Zacharias, *Small* **2007**, *3*, 1660; h) X. Liang, X. Wang, Y. Zhuang, B. Xu, S. Kuang, Y. Li, *J. Am. Chem. Soc.* **2008**, *130*, 2736; i) K. An, T. Hyeon, *Nano Today* **2009**, *4*, 359.
[3] C. M. Wang, D. R. Baer, L. E. Thomas, J. E. Amonette, J. Antony, Y. Qiang, G. Duscher, *J. Appl. Phys.* **2005**, *98*, 094308.
[4] a) Y. Yin, C. K. Erdonmez, A. Cabot, S. Hughes, A. P. Alivisatos, *Adv. Funct. Mater.* **2006**, *16*, 1389; b) A. Cabot, V. F. Puntes, E. Shevchenko, Y. Yin, L. Balcells, M. A. Marcus, S. M. Hughes, A. P. Alivisatos, *J. Am. Chem. Soc.* **2007**, *129*, 10358.
[5] a) H. J. Fan, M. Knez, R. Scholz, D. Hesse, K. Nielsch, M. Zacharias, U. Gösele, *Nano. Lett.* **2007**, *7*, 993; b) R. Nakamura, G. Matsubayashi, H. Tsuchiya, S. Fujimoto, H. Nakajima, *Acta Mater.* **2009**, *57*, 5046.
[6] A. Cabot, R. K. Smith, Y. Yin, H. Zheng, B. M. Reinhard, H. Liu, A. P. Alivisatos, *ACS Nano* **2008**, *2*, 1452.
[7] R. Nakamura, J.-G. LEE, H. Mori, H. Nakajima, *Philos. Mag.* **2008**, *88*, 257.
[8] a) A. Maezawa, Y. Okamoto, T. Imanaka, *J. Chem. Soc., Faraday Trans 1* **1987**, *83*, 665; b) Y. Yang, D. S. Kim, M. Knez, R. Scholz, A. Berger, E. Pippel, D. Hesse, U. Gösele, M. Zacharias, *J. Phys. Chem. C* **2008**, *112*, 4068.
[9] K. Ellmer, A. Klein, B. Rech, in *Transparent Conductive Zinc Oxide: Basics and Applications in Thin Film Solar Cells* (Ed: K. Ellmer, A. Klein, B. Rech), Springer, Heidelberg, Germany **2008**, pp. 21–23.
[10] a) G. W. Tomlins, J. L. Routbort, T. O. Mason, *J. Am. Ceram. Soc.* **1998**, *81*, 869; b) A. Birnboim, T. Olorunyolemi, Y. Carmel, *J. Am. Ceram. Soc.* **2001**, *84*, 131.
[11] P.Shewmon, in *Diffusion in Solids*, 2nd ed., The Minerals, Metals and Materials Society, Warrendale, PA **1989**, pp. 30–34.
[12] W. D. Pilkey,R. E. Peterson, in *Peterson' Stress Concentration Factors*, 2nd ed., Wiley, Weinheim, Germany **1997**, pp. 1–508.
[13] M. Keplinger, T. Mårtensson, J. Stangl, E. Wintersberger, B. Mandl, D. Kriegner, V. Holý, G. Bauer, K. Deppert, L. Samuelson, *Nano Lett.* **2009**, *9*, 1877.
[14] a) S. Hoffmann, F. Oestlund, J. Michler, H. J. Fan, M. Zacharias, S. H. Christiansen, C. Ballif, *Nanotechnology* **2007**, *18*, 205503; b) H. Markoc, U. Ozgur, *Zinc Oxide: Fundementals, Materials, Device Technology*, Wiley, Weinheim **2009**, p. 50; c) W. S. Yang, Y. K. Kim, S.-Y. Yang, J. H. Choi, H. S. Park, S. I. Lee, J.-B. Yoo, *Surf. Coat. Tech.* **2000**, *131*, *79*; d) C. F. Hermann, F. W. DelRio, D. C. Miller, S. M. George, V. M. Bright, J. L. Ebel, R. E. Strawser, R. Cortez, K. D. Leedy, *Sens. Actuators A* **2007**, *135*, 262; e) G. Stan, C. V. Ciobanu, P. M. Parthangal, R. F. Cook, *Nano Lett.* **2007**, *7*, 3691; f) G. Simmons, H. Wang, *Single Crystal Elastic Constants and Calculated Aggregate Properties: A Handbook*, 2nd ed, M.I.T. Press, Cambridge, MA, USA **1971**, p. 146.
[15] Y. Yang, R. B. Yang, H. J. Fan, R. Scholz, Z. Huang, A. Berger, Y. Qin, M. Knez, U. Gösele, *Angew. Chem.* **2010**, *122*, 1484; *Angew. Chem. Int. Ed.* 2010, *49*, 1442.
[16] B. Zhang, Y. Jung, H.-S. Chung, L. V. Vugt, R. Agarwal, *Nano Lett.* **2009**, *10*, 149.
[17] C. C. Büttner, M. Zacharias, *Appl. Phys. Lett.* **2006**, *89*, 263106.

Received: April 6, 2010
Published online: July 15, 2010

